The Journal of Neuroscience, June 1992, 12(6): 2288–2302

Spatial and Temporal Expression of α- and β-Thyroid Hormone Receptor mRNAs, Including the β_2-Subtype, in the Developing Mammalian Nervous System

David J. Bradley,[1,2] Howard C. Towle,[2] and W. Scott Young III[1]

[1]Laboratory of Cell Biology, National Institute of Mental Health, National Institutes of Health, Bethesda, Maryland 20892 and [2]Department of Biochemistry, University of Minnesota, Minneapolis, Minnesota 55455

Thyroid hormone exerts profound effects on the developing mammalian brain, and its deficiency can lead to severe mental retardation and motor abnormalities. To identify specific anatomic targets of thyroid hormone action in the developing mammalian nervous system, we examined thyroid hormone receptor gene expression by hybridization histochemistry on serial adjacent sections from 12 stages of the developing rat nervous system. ^{35}S-labeled cRNA probes were generated from divergent sequences of rat α_1-, α_2-, β_1-, and β_2-thyroid hormone receptor and related cDNAs. We found that α- and β-thyroid hormone receptor genes have distinct patterns of spatiotemporal expression in the embryonic and postnatal rat nervous system. α_1- and α_2- mRNAs were widely expressed in similar patterns; highest levels were found in the fetal neocortical plate, site of cortical neuronal differentiation. In contrast, β_1-transcripts were restricted in distribution, with prominent expression in zones of neuroblast proliferation such as the germinal trigone and the cortical ventricular layer. Surprisingly, the "pituitary-specific" β_2-transcript was detected in the developing hippocampus and striatum. Our results suggest that α- and β-thyroid hormone receptors may play distinct functional roles during development of the mammalian nervous system.

Differential regulation of transcription is widely viewed as one of the principal mechanisms guiding mammalian brain development. cDNAs encoding numerous transcription factors have been cloned, and many of these regulatory proteins have been found to be expressed in the developing CNS (He and Rosenfeld, 1991; Struhl, 1991). Their contributions to neuronal proliferation, determination of cell lineages, and establishment of interneuronal connections are just beginning to be elucidated. One group of transcription factors likely to play a crucial role in events such as these are thyroid hormone receptors. Thyroid hormone deficiency in developing humans is associated with irreversible mental retardation and profound neurologic deficits including movement disorders and deafness (DeLong, 1989). Experimentally induced thyroidectomy around the time of birth in rats causes numerous neurologic abnormalities including diminished interneuronal connectivity (Eayrs, 1955), decreased myelination, and alterations in levels of neurotransmitters such as norepinephrine and dopamine (Dussault and Ruel, 1987).

Thyroid hormone binds to receptors that belong to an extended family of ligand-dependent transcription factors that includes nuclear receptors for steroid hormones and retinoic acid (Glass and Holloway, 1990; Brent et al., 1991). Members of the nuclear receptor superfamily are thought to share a common mechanism of action in which hormone-receptor complexes bound to *cis*-acting DNA elements enhance or repress transcription of target genes (Evans, 1988). Thyroid hormone receptors are encoded by two genes, α and β c-*erbA* (Sap et al., 1986; Weinberger et al., 1986). In rat, these genes give rise to three functional thyroid hormone receptors: α_1, β_1, and β_2 (Thompson et al., 1987; Izumo and Mahdavi, 1988; Koenig et al., 1988; Murray et al., 1988; Hodin et al., 1989). Alternative splicing of the rat c-*erbA*α (rc-*erbA*α) RNA generates 3′ variant transcripts, referred to here collectively as rc-*erbA*α_2 mRNA (Izumo and Mahdavi, 1988; Lazar et al., 1988; Mitsuhashi et al., 1988; Mitsuhashi and Nikodem, 1989). Unlike functional thyroid hormone receptors, rc-*erbA*α_2 protein products fail to bind thyroid hormone or regulate gene expression in a thyroid hormone–dependent manner (Izumo and Mahdavi, 1988; Lazar et al., 1988; Mitsuhashi et al., 1988). Northern analysis has demonstrated rc-*erbA*α_1 (α_1), rc-*erbA*α_2 (α_2), and rc-*erbA*β_1 (β_1) mRNA expression in many adult rat tissues (Thompson et al., 1987; Koenig et al., 1988; Mitsuhashi et al., 1988; Murray et al., 1988; Hodin et al., 1989, 1990; Mitsuhashi and Nikodem, 1989). In contrast, rc-*erbA*β_2 (β_2) mRNA, which differs from the β_1-transcript at its 5′ end, has previously been detected only in the pituitary of adult rats (Hodin et al., 1989, 1990; Cook and Koenig, 1990).

Northern analysis and PCR have revealed differential accumulation of α_1-, α_2-, and β_1-transcripts in the whole and dissected developing rat brain (Mitsuhashi and Nikodem, 1989; North and Fisher, 1990; Strait et al., 1990, 1991; Wills et al., 1991). Analogous trends have been found in amphibian (Yaoita and Brown, 1990) and avian development (Forrest et al., 1990, 1991). The anatomic details, however, of c-*erbA* expression during development of the mammalian nervous system have remained unknown, and although thyroid hormone binding sites are present in rat embryos as early as embryonic day 14 (E14) (Perez-Castillo et al., 1985), previous studies have not examined c-*erbA* expression during the critical stages of rat brain maturation that

Received Oct. 21, 1991; revised Jan. 14, 1992; accepted Jan. 15, 1992.

We thank M. Brownstein for primer synthesis; L. Brady, A. Lynn, E. Shepard, and H. Whitfield for technical assistance; and E. Farr, C. Gerfen, J. McClaskey, and C. Weinberger for helpful discussions. We are indebted to M. Lazar and W. Chin for generously providing c-*erbA*β_2 PCR template and M. Lazar for GH3 RNA. We also thank M. Herkenham for helpful discussions about developmental neuroanatomy and R. Dreyfuss for expert photographic assistance. D.J.B. was supported by the Howard Hughes Medical Institute during the initial stages of this work. D.J.B. is a fellow of the Medical Scientist Training Program.

Correspondence should be addressed to W. Scott Young III, M.D., Ph.D., National Institutes of Health, Building 36, Room 2D10, Bethesda, MD 20892.

occur prior to E19. In addition, studies of β_2 c-*erbA* expression in rats have been confined to adult tissues (Hodin et al., 1989, 1990; Cook and Koenig, 1990).

A detailed direct comparison of the spatial and temporal expression patterns of α_1, α_2, β_1, and β_2 c-*erbA* mRNAs in the developing mammalian brain should provide insight into the developmental cues driving transcription of thyroid hormone receptor genes and may suggest distinct functional roles for the corresponding gene products. We have used hybridization histochemistry to accomplish this goal. ^{35}S-cRNA probes specific for each of the four principal subtypes of rat c-*erbA* transcripts were prepared. These probes were applied to over 3000 serial adjacent sections collected in coronal, transverse, and sagittal planes from 12 stages of rat brain development ranging from E11.5 (midgestation) to 9 weeks postnatally (early adulthood). Our results show that rc-*erbA* α- and β-genes have distinct ontogenetic expression domains. The presence of three (i.e., α_1, β_1, as well as β_2) rather than two functional thyroid hormone receptor mRNAs in the developing CNS suggests a previously unrecognized level of complexity in thyroid hormone regulation of brain development.

Materials and Methods

Tissue preparation. Timed-pregnant Sprague–Dawley rats (Taconic Farms) were killed by decapitation and their uterine horns transferred to 4°C 1× PBS for dissection. Noon of the vaginal plug day and the day of birth were designated E0.5 and P0, respectively. Embryonic ages between E11.5 and E19.5 were confirmed by crown–rump measurements (Hebel and Stromberg, 1986). Embryos plus uteri (E11.5, E12.5) or embryos alone (E13.5, E15.5, E17.5, E19.5) were snap frozen in −20°C isopentane and stored at −80°C. P0, P4, P7, and P11 heads and P21 and 9 week brains were similarly frozen and stored. Serial 12-μm-thick frozen tissue sections in sagittal (all stages), transverse (E12.5, E13.5), and coronal (E15.5, E17.5, E19.5, P0, P4, P7, P11, P21, 9 week) planes were collected on chrom-alum–subbed slides at −18°C in groups of six adjacent sections: one for Nissl staining, four for antisense cRNA probes, and one for sense control cRNA probe. Additional adjacent coronal sections from the diencephalon were collected for corticotropin-releasing factor (CRF), thyrotrophin-releasing hormone (TRH), and sense oligonucleotide probes. Slides and tissue sections were stored at −80°C prior to pretreatment.

Plasmid constructions. Polymerase chain reaction was used to amplify divergent regions of rat c-*erbA* cDNAs: nucleotides 1437–1886 of rc-*erbA*α_1 (Thompson et al., 1987), nucleotides 1923–2378 of rc-*erbA*α_2 (Lazar et al., 1988), nucleotides −206–183 of rc-*erbA*β_1 (Murray et al., 1988), and nucleotides 110–491 of rc-*erbA*β_2 (Hodin et al., 1989). Following treatment with T4 kinase, the resulting PCR products were subcloned into the HincII site of pGEM3Z (Promega), generating plasmids pGTRα_1, pGTRα_2, pGTRβ_1, and pGTRβ_2. Insert orientations were determined by restriction mapping, and fidelity of amplifications was confirmed by dideoxy sequencing (Sanger et al., 1977). Templates for generating antisense cRNA probes were prepared by linearizing pGTRα_1 and pGTRβ_1 with two rounds of EcoRI digestion and pGTRα_2 and pGTRβ_2 with two rounds of HindIII digestion. Sense control cRNA probes were generated from a template containing nucleotides 81–528 of the rat glucocorticoid receptor cDNA (Arriza et al., 1988).

cRNA probe labeling. ^{35}S-labeled cRNA probes were transcribed from templates using 20 μM ^{35}S-UTP (New England Nuclear; 1000–1500 Ci/mmol) and either SP6 (α_1, β_1) or T7 (α_2, β_2, sense) RNA polymerases. Probes labeled with both ^{35}S-UTP and ^{35}S-CTP produced unacceptably high background. Probes were reduced to approximately 160 nucleotides by limited alkaline hydrolysis at pH 10.2 (Cox et al., 1984). Average sizes of hydrolyzed probes were confirmed by polyacrylamide gel electrophoresis.

cRNA hybridization histochemistry. Prior to hybridization, tissue sections were pretreated essentially as described (Young, 1990). Briefly, sections were warmed at room temperature for 10 min, fixed in 4% formaldehyde, 1× PBS for 5 min, rinsed twice in 1× PBS, and acetylated in 0.1 M triethanolamine-HCl (pH 8), 0.25% acetic anhydride for 10 min. Sections were then rinsed twice in 2× saline–sodium citrate (SSC); dehydrated in 70% (1 min), 80% (1 min), 95% (2 min), and 100% (1 min) ethanol; delipidated in 100% chloroform (5 min); and partially rehydrated in 100% (1 min) and 95% (1 min) ethanol prior to air drying.

cRNA hybridization histochemistry was based on procedures of Cox et al. (1984) and Whitfield et al. (1990). ^{35}S-cRNA probes were denatured at 65°C for 5 min and placed on ice for 5 min. Final hybridization buffer, with 1×10^6 cpm of denatured α^{35}S-cRNA probe per 50 μl, consisted of 20 mM Tris-HCl (pH 7.4), 1 mM EDTA (pH 8.0), 300 mM NaCl, 50% formamide, 10% dextran sulfate, 1× Denhardt's, 25 mg/ml yeast *t*RNA, 100 μg/ml salmon sperm DNA, 250 μg/ml total yeast RNA (fraction XI, Sigma), 100 mM dithiothreitol (DTT), 0.1% sodium thiosulfate, and 0.1% SDS. We compared hybridization results using 1×10^5, 2×10^5, 5×10^5, 1×10^6, and 5×10^6 cpm cRNA rc-*erbA* probes per 50 μl of hybridization buffer and found 1×10^6 cpm/50 μl produced maximum signal : noise ratios. Addition of 50 μM α-thio-UTP to the hybridization buffer did not appreciably reduce background. Hybridization buffer (70 μl/1000 μm^2) was applied to sections on each slide and covered with untreated glass coverslips (Thomas Scientific). Slides were then incubated at 56°C in chambers humidified with 2× SSC/50% formamide. In preliminary experiments, hybridization times were varied between 16 h and 24 h; 24 h was found to produce the best signal : noise ratio.

Following hybridization, slides were cooled to room temperature, and coverslips were floated off slides in 4× SSC. Slides were then washed essentially as described (Simmons et al., 1989). Briefly, slides were rinsed in four rounds of 4× SSC followed by immersion in 20 μg/ml RNase A (Boehringer Mannheim) at 37°C for 30 min. Sections were then desalted in graded SSC solutions and washed twice in 0.1× SSC at 65°C for 30 min each. After dehydration in graded alcohol solutions containing 300 mM ammonium acetate and 1 mM DTT, sections were air dried.

Oligonucleotide hybridization histochemistry. ^{35}S-Labeled 48 base oligodeoxyribonucleotide probes complementary to rat CRF mRNA (Young et al., 1986a) and rat TRH mRNA (Koller et al., 1987) and homologous to rat vasopressin mRNA (Young et al., 1986b) (sense, control) were used as markers to identify the fetal hypothalamic paraventricular nucleus (PVN). Oligonucleotide hybridization histochemistry was performed as previously described (Young, 1990) on sections pretreated as above.

Autoradiography and image analysis. Slides were apposed to Amersham Hyperfilm-βmax for 4–16 d. Slides were then coated with nuclear track emulsion (NTB-2, Kodak) diluted 1:1 in 600 mM ammonium acetate. Following exposure of 6–10 weeks at −20°C, slides were developed in D-19 (Kodak) and counterstained with thionin. Sections that included a given region (e.g., hypothalamus) were identically pretreated, hybridized, washed, exposed, developed, and stained.

Standardized image analysis of autoradiographic signals was performed according to Young (1990). Briefly, autoradiographic signals were measured using Image, a Macintosh-based image analysis system (W. Rasband, NIH). Optical densities were converted to dpm/mg using coexposed ^{35}S brain paste standards. This allowed correction for the nonlinear response of film to radioactivity.

Northern analysis. Total brain RNA from adult male Sprague–Dawley rats was isolated by centrifugation in cesium trifluroacetate (Cs-TFA) as described (Okayama et al., 1987). Brain RNA and GH3 RNA (generous gift of M. Lazar, University of Pennsylvania) were then transferred to GeneScreen according to Koller et al. (1987). Blots were prehybridized for 16 hr at 65°C in 50% formamide, 4× SSPE, 10% dextran sulfate, 4× Denhardt's, 200 μg yeast *t*RNA/ml, 200 μg total yeast RNA (fraction XI, Sigma)/ml, and 0.1% SDS. Following prehybridization, blots were transferred to hybridization buffer consisting of fresh prehybridization buffer plus ^{32}P-cRNA probes at a final concentration of 2×10^6 cpm/ml. cRNA probes were labeled with 3 μM ^{32}P-UTP (800 Ci/mmol; NEN) and 15 μM UTP. Hybridization was at 65°C for 24 hr. Blots were washed at a final stringency of 0.1× SSC/65°C, the same as that used for cRNA hybridization histochemistry.

Results

To assess the expression of various forms of c-*erbA* transcripts in the developing rat brain, a series of specific hybridization probes were developed. Divergent regions of α_1, α_2, β_1, and β_2 rat c-*erbA* cDNAs (Fig. 1*A*) were subcloned into plasmid pGEM to allow preparation of high-specific-activity ^{35}S-labeled cRNA

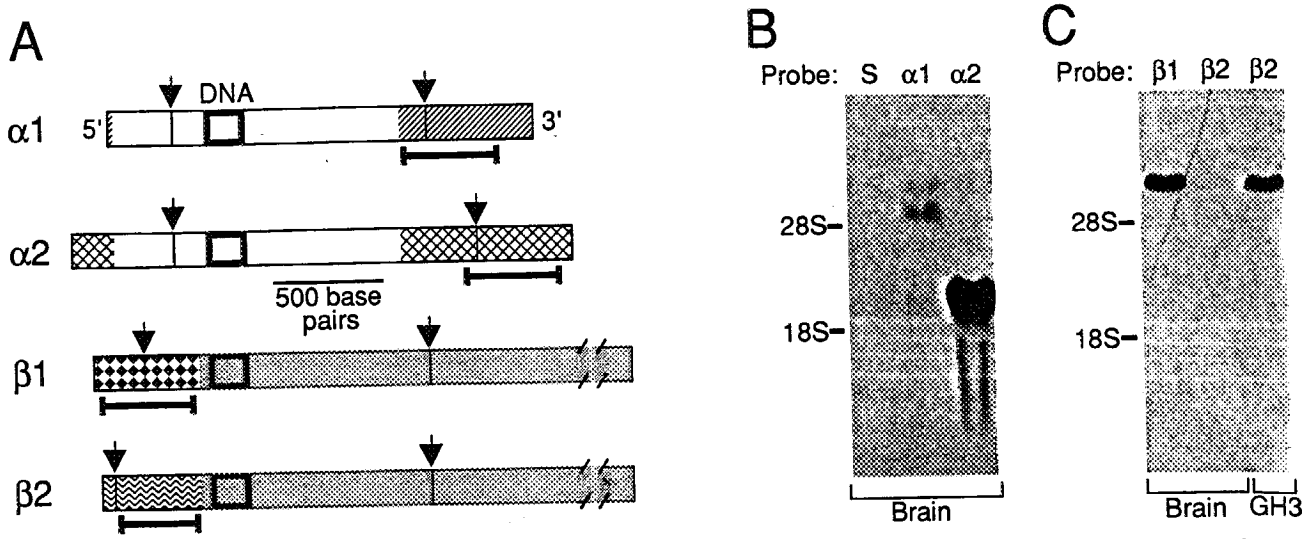

Figure 1. Probes for detection of c-*erbA* mRNAs by hybridization histochemistry. *A*, Schematic representations of α_1, α_2, β_1, and β_2 c-*erbA* cDNAs. Divergent sequences are indicated by *patterns* and *stippling*. Regions of cDNAs used to generate cRNA probes for hybridization histochemistry are indicated by *bars*. *Arrows* indicate translation initiation and termination codons, and *boxed areas* show putative DNA binding domains. *B* and *C*, Confirmation of cRNA probe hybridization specificity by Northern analysis. Twenty micrograms of total adult rat brain RNA (*Brain*) or 10 μg of total GH3 RNA (*GH3*) were loaded into each lane as indicated. The resulting blots were hybridized with either the probes shown in *A* or a sense control probe (*S*). Final wash stringency was identical to that used for hybridization histochemistry. Positions of 18S [1.9 kilobases (kb)] and 28S (4.8 kb) rRNA are shown. Exposure time: 4 d (*B* and *C*).

probes. When the resulting probes were hybridized to blots of total RNA from adult rat brain and GH3 cells (an anterior pituitary tumor cell line), bands of characteristic, previously reported sizes were detected (Fig. 1*B,C*) (Mitsuhashi et al., 1988; Murray et al., 1988; Hodin et al., 1989, 1990; Mitsuhashi and Nikodem, 1989). Background levels were established using a sense probe that failed to hybridize to adult rat brain RNA by Northern analysis (Fig. 1*B*) and that produced negligible signal by hybridization histochemistry (e.g., Fig. 4). This sense probe was applied to contiguous adjacent tissue sections from all sites and stages examined. In adult rat brain, our cRNA probes generated by hybridization patterns in close agreement with those previously described using corresponding oligodeoxyribonucleotide probes (Bradley et al., 1989).

Hybridization histochemistry was initially performed on tissue from mid-gestation rat fetuses to assess c-*erbA* expression in the context of early brain development. C-*erbA* transcripts were detected as early as E11.5 (Table 1) when both α_1- and α_2-mRNAs were found at low levels in the neural tube. One day later (E12.5), a substantial increase in α_1- and α_2-labeling was found throughout the rostral neural tube in each of the five vesicles that form the precursors of the major subdivisions of the brain: tel-, di-, mes-, met-, and myelencephalon. Also on E12.5, β_1-transcripts were first detected, but in an expression domain restricted to the ventral rhombencephalon and the ventral diencephalon rostral to the optic sulcus. No β_2-signal was found at E12.5.

Table 1 summarizes c-*erbA* mRNA levels in fetal brain, and Figures 2 and 3 provide an overview of c-*erbA* expression from E13.5 to 9 weeks postnatally. Throughout gestation and into early adulthood, α_1- and α_2-mRNAs were widely distributed in the CNS in a highly similar pattern, with α_2-transcripts generally more abundant than α_1-mRNAs (Fig. 2, 3). In contrast, β_1- and β_2-hybridization signals were far more limited in distribution. Consistent with our previous results in the adult rat brain (Bradley et al., 1989), the spatiotemporal β-expression domain appeared to be a subset of the α-domain. Below we describe in greater detail the distribution of c-*erbA* mRNAs in five brain regions that have particular relevance to thyroid hormone action in the developing brain and that highlight the distinct ontogenetic expression patterns of α and β c-*erbA* transcripts.

Striatum

Between E13 and E22, neuroblasts in the caudate-putamen (CPu) neuroepithelium (ventricular germinal zone) undergo terminal mitoses, and the resulting young neurons populate the developing striatum (Bayer, 1984). During this time, a striking difference in expression of rc-*erbAα* and rc-*erbAβ* arises. α_1- and α_2-labeling of the emerging CPu is prominent and generally uniform (Fig. 2). As early as E15.5, however, β_1-mRNAs are confined to the rostral striatum (Table 1), and a steep rostral-caudal gradient of β_1-expression arises that is especially prominent during the early postnatal period (Figs. 2–4). Whereas the rostral edge of this gradient conforms to the corresponding border of the striatum, the caudal limit of expression falls on no recognizable anatomic boundary (Fig. 4). Coronal sections further define the β_1-striatal gradient as dorsolateral to ventromedial (not shown). The steepness of the gradient diminishes following the first week postnatally.

A second striking result emerged from our study of the striatum. As shown in Figures 3 and 4, β_2-mRNAs, previously described as being detectable only in the pituitary (Hodin et al., 1989; Cook and Koenig, 1990), were found in the striatum at low specific levels in a gradient similar to that of β_1-transcripts. We have confirmed this result at other stages and in both sagittal and coronal planes (not shown).

Neocortex

On E13, newly postmitotic neurons within the neocortical ventricular layer begin to migrate radially outward (Raedler and

Table 1. C-*erbA* mRNA levels in the fetal rat nervous system and pituitary

	α1	α2	β1	β2
E11.5				
Neural tube	+	+	-	-
E12.5				
Telencephalon	++	++(+)	-	-
Diencephalon	+(+)	++	(+)	-
Mesencephalon	+(+)	++	+(+)	-
Metencephalon	+(+)	+(+)	+	-
Myelencephalon	+(+)	+(+)	+	-
E13.5				
Cortical ne	+++	+++	-	-
Basal telencephalon	+(+)	++	-	-
Hippocampal ne	++	++(+)	-	-
Thalamic ne	++(+)	++++	-	-
Hypothalamic ne	+(+)	++	(+)	-
Tegmental ne	+	+(+)	+	-
Superior colliculus ne	+	+	(+)	-
Inferior colliculus ne	+	+	-	-
Pons	+	++(+)	-	-
Medulla	+	++(+)	-	-
Cerebellar ne	+	+(+)	-	-
Trigeminal ganglion	+(+)	+++	-	-
Facial ganglion	++	++++	-	-
Vestibular ganglion	++	++++	-	-
Dorsal root ganglion	+(+)	+++	(+)	-
Spinal cord	++	++(+)	-	-
Anterior pituitary	+(+)	+(+)	++(+)	+
E15.5				
Olfactory bulb ne	+++	++++	-	-
Neocortex				
Ventricular layer	+	+(+)	+	-
Intermediate layer	+	+	-	-
Cortical Plate	++++	++++	-	-
Layer I	(+)	(+)	-	-
Piriform cortex	++(+)	++(+)	+	-
Septal ne	+	+(+)	+	-
Caudate putamen ne	++(+)	+++	-	-
Caudate putamen rostral	++(+)	++++	+(+)	-
Caudate putamen caudal	++(+)	++++	-	-
Hippocampal ne	++	++	(+)	-
Hippocampus	++++	++++	-	-
Thalamus	+++	++++	-	-
Anterior hypothalamic a	+++	++++	-	-
Tegmentum	++(+)	++++	-	-
Upper tegmental ne	+(+)	++	++(+)	(+)
Superior colliculus	++	+++	+	-
Inferior colliculus	++	+++	-	-
Pons	+(+)	++++	-	-
Medulla	+(+)	++++	-	-
Vestibular n	+	++	-	-
Facial n	+(+)	++	(+)	-
Cerebellar ne	+++	++++	-	-
Cerebellar ctz	+++	+++	-	-
External germinal layer	(+)	(+)	-	-
Germinal trigone	++(+)	++(+)	++	-
Choroid plexus	+(+)	+(+)	+	-

E15.5 continued	α1	α2	β1	β2
Trigeminal ganglion	++(+)	+++	(+)	-
Vestibular ganglion	+(+)	++	(+)	-
Dorsal root ganglion	++	++++	(+)	-
Spinal cord	+++	++++	-	-
Anterior pituitary	+(+)	++	+(+)	+
E19.5				
Olfactory bulb ne	+++	++++	(+)	-
Neocortex				
Ventricular layer	+	+(+)	+(+)	-
Subventricular layer	+	+(+)	(+)	-
Intermediate layer	+	+	-	-
Inner cortical plate	+++	++++	(+)	-
Bipolar cortical plate	++++	++++	(+)	-
Layer I	(+)	(+)	-	-
Piriform cortex	++++	++++	+(+)	-
Caudate putamen ne	+++	++++	-	-
Caudate putamen rostral	++	++++	++(+)	+
Caudate putamen caudal	++	++++	-	-
Globus pallidus	++	+++	-	-
Hippocampal ne	++	++	+	-
Subiculum	++++	++++	++	(+)
CA1	++++	++++	+++	+
CA3	++++	++++	+(+)	-
Dentate gyrus	++++	++++	+	-
Thalamus	++(+)	++++	-	-
Hypothalamus				
Suprachiasmatic n	++(+)	++++	-	-
Supraoptic n	+	+++	-	-
Paraventricular n	++	++++	+	-
Anterior hypothalamic a	++	+++	-	-
VMH n	++(+)	++++	(+)	-
Arcuate n	++(+)	++++	-	-
Habenular n	++	++++	-	-
Amygdala	++(+)	++++	-	-
Tegmentum	+	++++	-	-
Superior colliculus	++	++++	-	-
Inferior colliculus	+++	++++	-	-
Sensory trigeminal n	+	++	(+)	-
Motor trigeminal n	+(+)	++(+)	(+)	-
Red n	+	++	(+)	-
Pontine n	+(+)	++++	-	-
Pontine reticular n	+	+++	-	-
Medial vestibular n	+(+)	++++	-	-
Gigantocellular reticular n	+(+)	++++	-	-
Inferior olive	++	++++	-	-
Cerebellar ne	+(+)	+++	+	-
Cerebellar ctz	+(+)	+++	-	-
Purkinje cell layer	+++	++++	-	-
External germinal layer	(+)	(+)	-	-
Germinal trigone	+++	++++	+	-
Choroid plexus	+(+)	++	-	-
Trigeminal ganglion	++(+)	++++	(+)	-
Vestibular ganglion	+(+)	++	-	-
Dorsal root ganglion	++(+)	++++	-	-
Spinal cord	+(+)	++++	-	-
Anterior pituitary	++	+++	+(+)	++++

+, Low (~10% of maximum); ++, moderate (~35%); +++, high (~60%); ++++, very high (~85%) film autoradiographic signals measured by standardized image analysis (see Materials and Methods for details). −, Signal less than or equal to sense control probe signal. (+), between − and +; +(+), between + and ++; ++(+), between ++ and +++. Signal level is a combination of transcript level per cell and the number of cells expressing a transcript in a given structure. Abbreviations: a, area; ctz, cortical transitory zone; n, nucleus; ne, neuroepithelium.

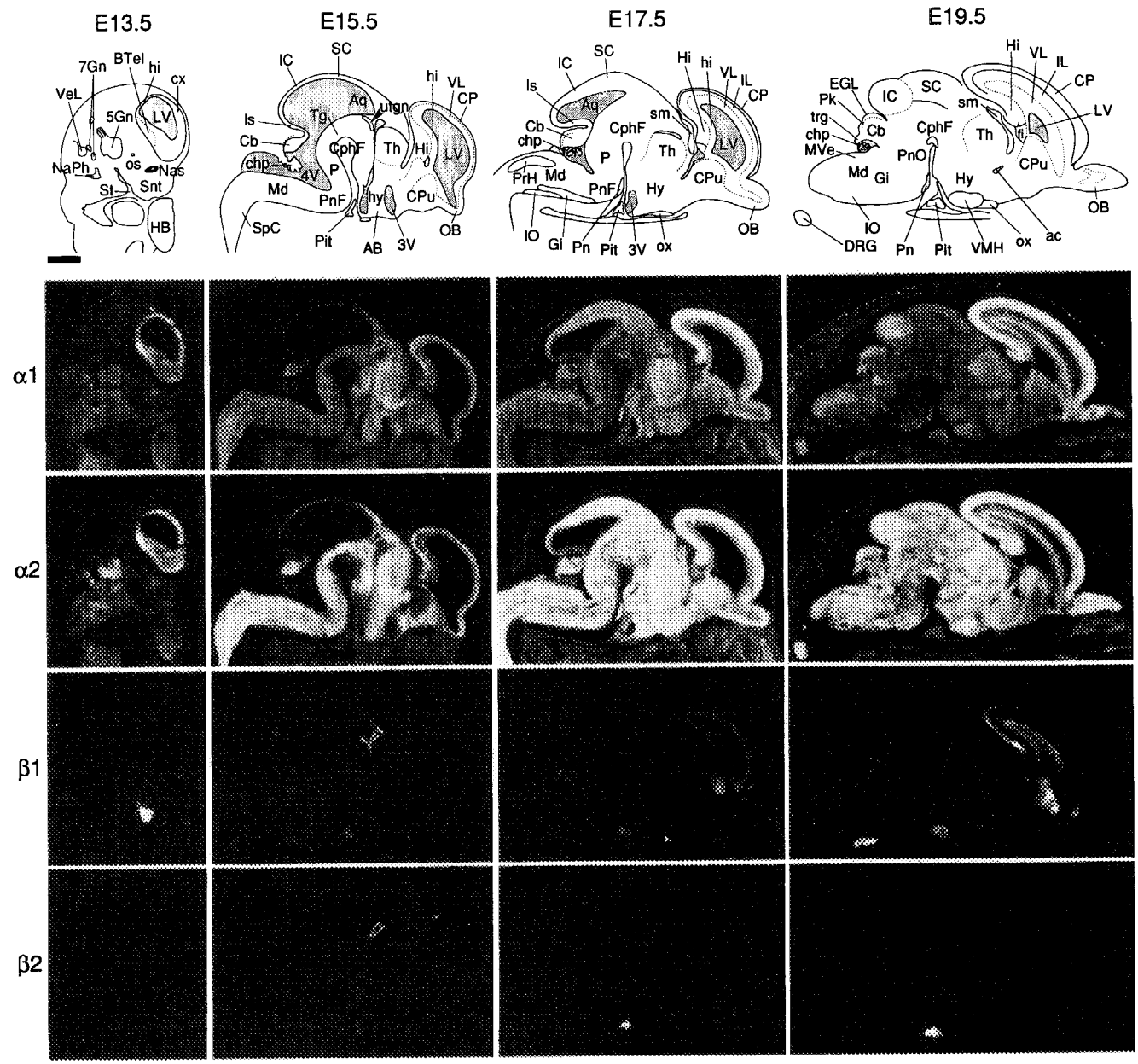

Figure 2. Overview of fetal expression of c-*erbA* transcripts in rat brain. Serial adjacent sagittal sections from E13.5, E15.5, E17.5, and E19.5 rats were hybridized with ^{35}S-labeled cRNA probes complementary to α_1, α_2, β_1, and β_2 rat c-*erbA* mRNAs. Sections were then apposed to film for 2 weeks. Higher levels of hybridization are *whiter*. Sections are shown schematically in *top row*. *Arrowheads* in E15.5 column indicate upper tegmental neuroepithelium. Abbreviations used here and in Figure 3 (n, nucleus; ne, neuroepithelium): *3V,* third ventricle; *4V,* fourth ventricle; *5Gn,* trigeminal ganglion; *5n,* trigeminal nerve; *7,* facial n; *7Gn,* geniculate ganglion; *AB,* anterobasal n; *ac,* anterior commissure; *Acb,* accumbens n; *AD,* anterodorsal thalamic n; *AH,* anterior hypothalamic area; *AOD,* anterior olfactory n, dorsal; *AOV,* anterior olfactory n, ventral; *AP,* anterior pituitary; *APT,* anterior pretectal n; *Aq,* aqueduct; *Arc,* arcuate n; *AV,* anteroventral thalamic n; *BTel,* basal telencephalon; *Cb,* cerebellum; *cc,* corpus callosum; *chp,* choroid plexus; *CP,* cortical plate; *CphF,* cephalic flexure; *CPu,* caudate putamen (striatum); *Cx,* cerebral cortex; *cx,* cortical ne; *DM,* dorsomedial hypothalamic n; *DRG,* dorsal root ganglion; *EGL,* external germinal layer, Cb; *fi,* fimbria hippocampus; *Gi,* gigantocellular reticular n; *GP,* globus pallidus; *HB,* hindlimb bud; *Hi,* hippocampal formation; *hi,* hippocampal ne; *Hy,* hypothalamus; *hy,* hypothalamic ne; Cx; *IC,* inferior colliculus; *IL,* intermediate layer; *IO,* inferior olive; *Is,* isthmus; *LDTg,* laterodorsal tegmental n; *LH,* lateral hypothalamic area; *LRt,* lateral reticular *n*; *LSO,* lateral superior olive; *LV,* lateral ventricle; *M,* mammillary nuclei; *Md,* medulla; *Me5,* mesencephalic trigeminal n; *Med,* medial cerebellar n; *Mo5,* motor trigeminal n; *MoCb,* molecular layer, Cb; *MVe,* medial vestibular n; *NaPh,* nasopharyngeal cavity; *Nas,* nasal cavity; *OB,* olfactory bulb; *os,* optic stalk; *ox,* optic chiasm; *P,* pons; *Pit,* pituitary; *Pk,* Purkinje cell layer, Cb; *Pk/IGL,* Purkinje cell layer/internal granular layer, Cb; *PMn,* paramedian reticular n; *Pn,* pontine nuclei; *PnC,* pontine reticular n, caudal; *PnF,* pontine flexure; *PnO,* pontine reticular n, oral; *PrH,* prepositus hypoglossal n; *R,* red nucleus; *Rt,* reticular thalamic n; *SC,* superior colliculus; *sm,* stria medullaris, Th; *SN,* substantia nigra; *Snt,* snout; *SO,* supraoptic n; *SpC,* spinal cord; *St,* stomodeum; *Tg,* tegmentum; *Th,* thalamus; *trg,* germinal trigone; *Tu,* olfactory tubercle; *utgn,* upper tegmental ne; *Ve,* vestibular nuclei; *VeL,* vestibular labyrinth; *VL,* ventricular layer; *VMH,* ventromedial hypothalamic n. Scale bar, 1 mm.

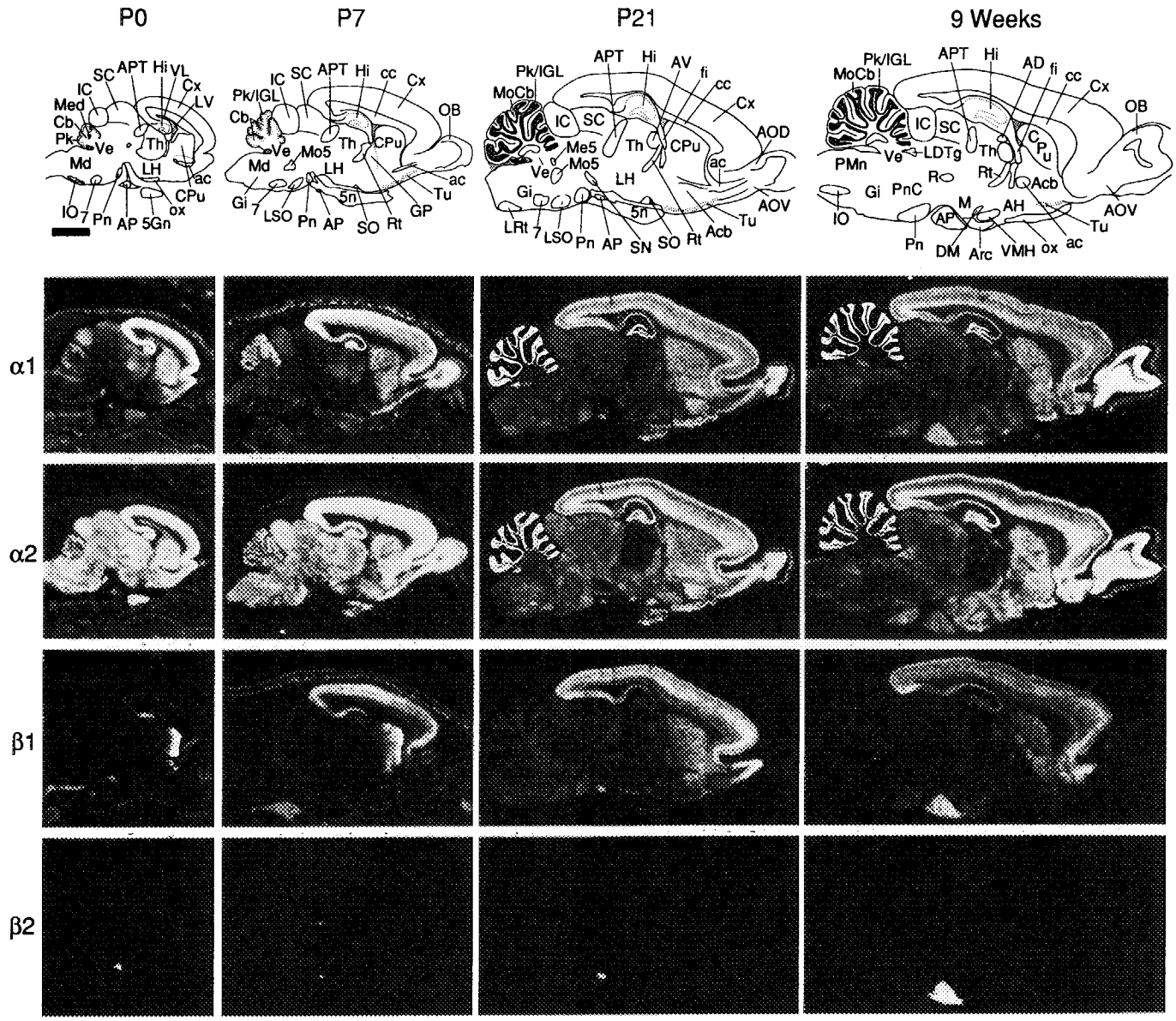

Figure 3. Overview of postnatal expression of c-*erbA* transcripts in rat brain. Serial adjacent sagittal sections from P0 and P7 rat heads and P21 and 9-week-old rat brains were hybridized with α_1, α_2, β_1, and β_2 rat c-*erbA* probes and apposed to film for 14 d. Anatomy is depicted schematically in *upper row.* See Figure 2 for abbreviations. Scale bar, 2.5 mm.

Raedler, 1978). Continued neuronal migration leads to the formation of three cortical layers that are first recognized on E15.5: cortical layer 1; the cortical plate (CP), precursor of definitive cortical layers 2–6; and the intermediate layer, which consists of afferent axons and neurons migrating outward from the ventricular layer to the CP (Fig. 5). Outward migration of young neurons to the E15.5 CP is associated with a surge in rc-*erbA*α mRNA levels (Fig. 5). This heightened expression in the CP continues through E19.5, when the CP is divided into the more superficial bipolar CP, to which postmitotic undifferentiated neurons initially migrate, and the inner CP, site of earliest anatomic differentiation of cortical neurons. Increased α_1- and α_2-mRNA signal in the E15.5 and E19.5 CPs does not merely reflect high cell density in the CP, since the ventricular layer and outer CP have virtually identical cell densities (Raedler et al., 1980). In contrast to the E15.5 and E19.5 α-neocortical expression patterns, cortical β-transcripts are mainly confined to the ventricular layer, site of neuroblast proliferation (Fig. 5).

By P4 all six cortical layers are present (Fig. 5), and ongoing neuronal differentiation is accompanied by a rapid increase in the population of cortical macroglia (Hicks and D'Amato, 1968). Figure 5 shows that on P4, relatively high levels of α_1- and α_2-mRNAs are present throughout the width of the cortex, with layers 2 and 3 being most intensely labeled. In contrast, β_1-transcripts are largely restricted to midcortical layers, and as in the CPu, low levels of β_2-mRNAs are found in a pattern similar to that of β_1-transcripts. This same pattern is reflected in the young adult (Fig. 5), in which β_1-probes label cells in layer 5 of the parietal cortex most intensely. As we have noted previously (Bradley et al., 1989), α-mRNA distribution in the adult neocortex is distinct from that of β, with α_1- and α_2-transcripts concentrated in layers 2, 3, 5, and 6.

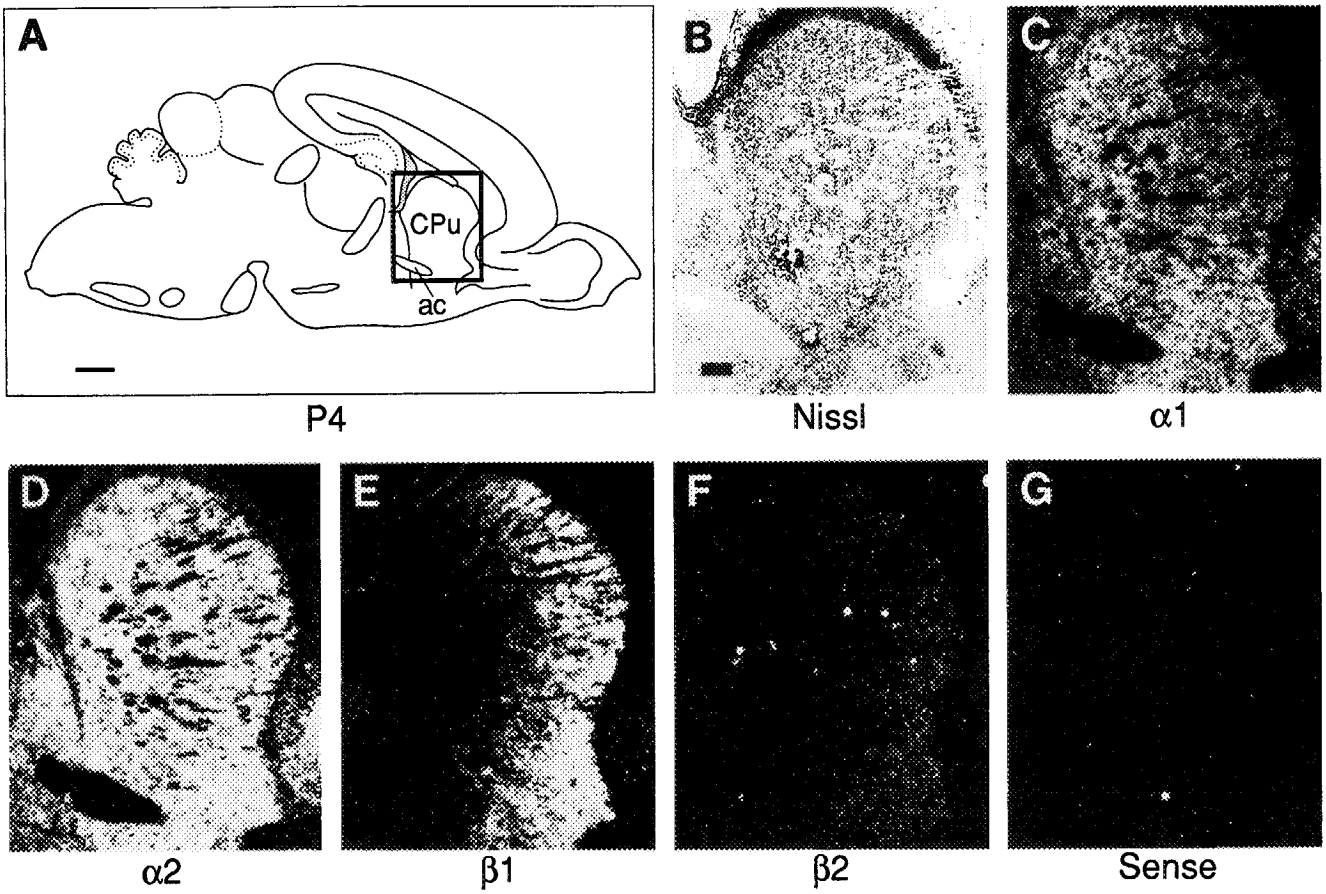

Figure 4. Differential expression of α and β c-*erbA* transcripts in P4 CPu. *A*, Illustration of P4 sagittal brain section. Area corresponding to *boxed region* is shown in *B–G*. *CPu*, caudate-putamen; *ac*, anterior commissure. *B–G*, Bright-field (*B*) and dark-field (*C–G*) photomicrographs of serial adjacent sagittal sections through the CPu. Following hybridization with either α_1, α_2, β_1, or β_2 rc-*erbA* probes or a sense control probe, sections were coated with photographic emulsion. Exposure time was 8 weeks. Labeled areas appear *white*. Rostral is to the right. Scale bars: thin bar, 1 mm; thick bar, 200 μm.

Hippocampus

On E15.5, the primordial hippocampus bulges from the dorsomedial wall of the telencephalon into the lateral ventricle (Fig. 6). Neurons populating Ammon's horn and the subiculum arise in the hippocampal ventricular germinal zone between E15 and E19 (Bayer, 1980). As in the developing neocortex, these postmitotic hippocampal neurons migrate to a relatively superficial position, where they begin to differentiate. On E15.5, we observed a superficial hippocampal cell layer intensely labeled with α_1- and α_2-probes (Fig. 6). This layer is continuous dorsally with the neocortical cortical plate, suggesting that, as in neocortical development, outward migration of postmitotic neurons from the hippocampal ventricular germinal zone is associated with a dramatic rise in α-mRNA levels. In contrast, only weak β_1-labeling of the E15.5 hippocampal neuroepithelium was found, and no β_2-labeling of this region above background was observed.

By P0, both the proliferating neuroblasts of the dentate primordium and their postmitotic daughter cells in the inner limb of the dentate gyrus granule cell layer were heavily labeled by α_1- and α_2-probes (Fig. 6). High levels of α-mRNAs were also present throughout the pyramidal cell layer of the P0 subiculum and Ammon's horn, whereas prominent labeling by β_1- and β_2-probes was restricted to the pyramidal cell layer of the subiculum and CA1.

Although dentate granule cells continue proliferating into adulthood (Bayer et al., 1982), the P11 hippocampal formation showed c-*erbA* expression very similar to that of the adult (Fig. 6). Heavy labeling by α_1- and α_2-probes of Ammon's horn and the dentate gyrus was found. In contrast, β_1-expression differed from that of α_1 and α_2, with highest β_1-labeling in CA1. In the dentate gyrus, only cells on the superficial and basal margins of the dentate granular layer had relatively high levels of β_1-mRNA. At P11, β_2-mRNAs were found in a distribution similar to that of β_1-transcripts, but at lower intensity.

Hypothalamus

The important role of thyroid hormone (T3) in the feedback regulation of TRH synthesis in the hypothalamic PVN (Koller et al., 1987; Segerson et al., 1987) prompted us to correlate thyroid hormone receptor and TRH gene expression in the developing PVN. TRH mRNA is first detected in cells of the lateral hypothalamus on E14 and in the primordial PVN on E16 (Burgunder and Taylor, 1989). Using probes for CRF and TRH mRNAs as markers for the developing PVN, we first detected c-*erbA* transcripts in the PVN on E17.5 (not shown). Figure 7*A–H* shows that on E19.5 both α_1- and α_2-probes heavily labeled

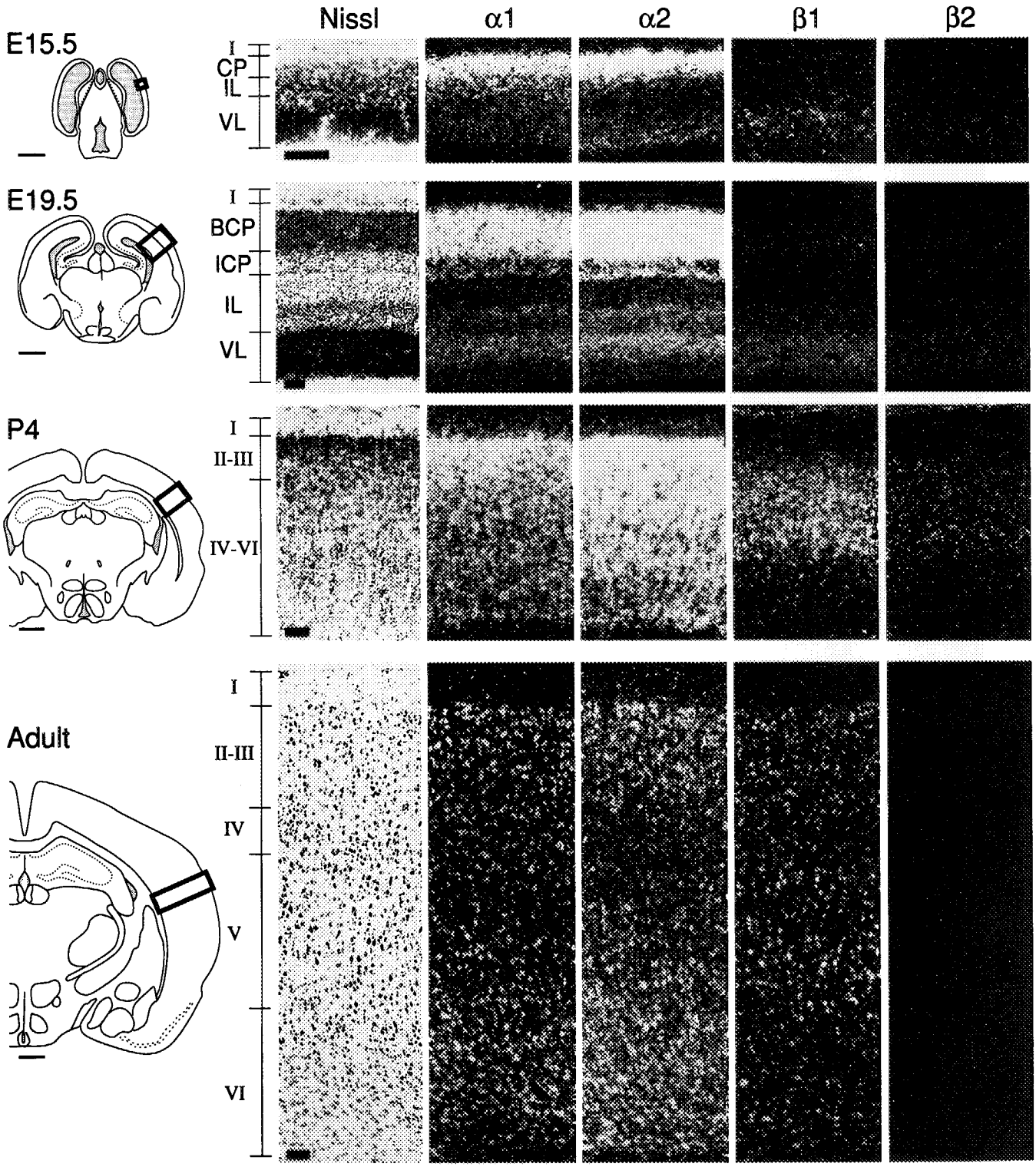

Figure 5. Distinct distributions of α and β c-*erbA* transcripts in the developing cerebral cortex. Serial adjacent coronal sections from E15.5, E19.5, P4, and 9 week (*Adult*) rat brains were hybridized with α_1, α_2, β_1, and β_2 rc-*erbA* probes and coated with photographic emulsion. Sections are illustrated schematically in the *left column.* Bright-field (*Nissl*) and dark-field photomicrographs of cortical areas outlined by *boxes in left column* are shown in remaining columns. Cortical layers at each stage are indicated. Exposure time was 10 weeks. *BCP,* bipolar cortical plate; *CP,* cortical plate; *ICP,* inner cortical plate; *IL,* intermediate layer; *VL,* ventricular layer; *I, II, III, IV, V, VI,* layers of neocortex. Scale bars: thin bars, 1 mm; thick bars, 100 μm.

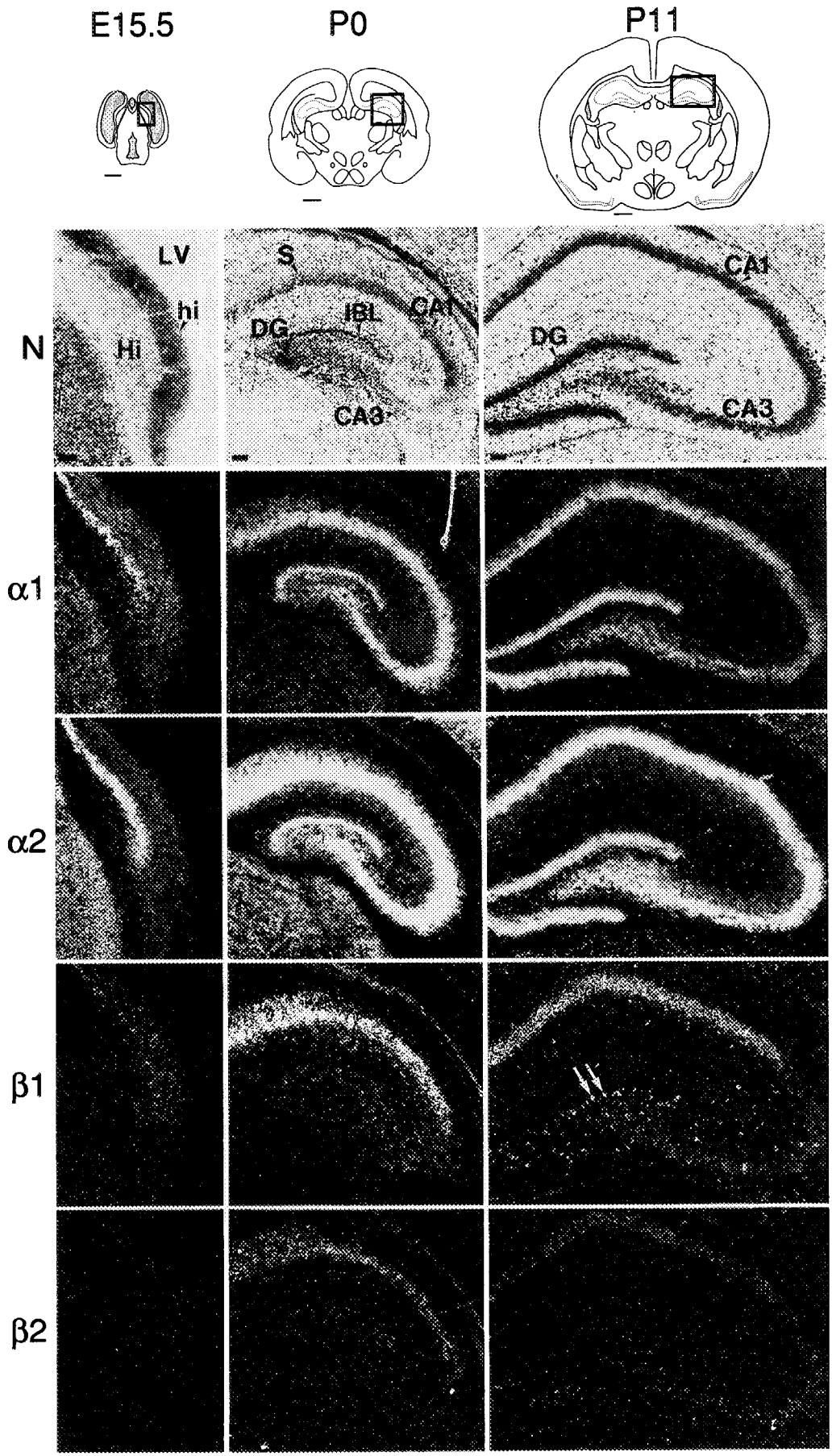
E15.5
P0
P11
N
α1
α2
β1
β2
LV
hi
Hi
S
IBL
DG
CA1
CA3

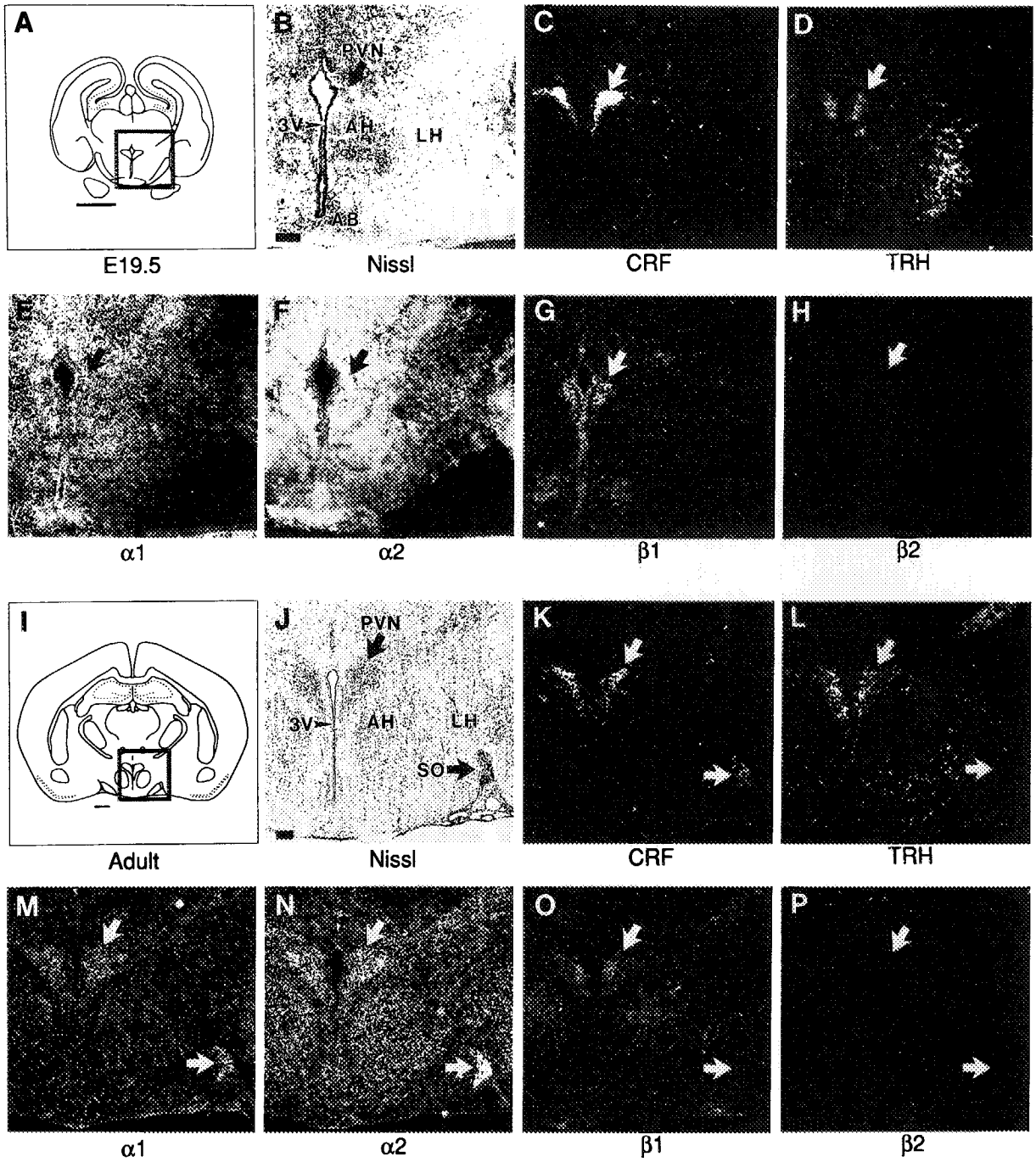

Figure 7. Comparison of c-*erbA*, CRF, and TRH mRNA distributions in fetal and adult rat hypothalamus. *A* and *I*, Schematic illustrations of coronal sections through the hypothalamus of E19.5 and adult rat brain. Bright-field (*B*) and dark-field (*C–H*) photomicrographs of adjacent sections correspond to *boxed region in A*. Similarly, bright-field (*J*) and dark-field (*K–P*) photomicrographs of adjacent adult sections correspond to *boxed region in I*. Serial adjacent sections were hybridized with α_1, α_2, β_1, and β_2 rc-*erbA* cRNA probes and CRF and TRH oligonucleotide probes as indicated. Sections were then coated with photographic emulsion. Exposure times were 5 (*C, D, K, L*) or 10 (*E–H, M–P*) weeks. *3V*, third ventricle; *AB*, anterobasal nucleus; *AH*, anterior hypothalamic area; *LH*, lateral hypothalamic area; *PVN*, paraventricular hypothalamic nucleus; *SO*, supraoptic nucleus. Scale bars: thin, 1 mm; thick, 200 μm.

←

Figure 6. α_1, α_2, β_1, and β_2 rc-*erbA* transcripts in the developing rat hippocampal formation. *Top row*, Schematic illustrations of E15.5 P0, and P11 coronal sections. Photomicrographs corresponding to *boxed areas in top row* are shown below. Bright-field (*Row N*) and dark-field (*rows* α_1, α_2, β_1, *and* β_2) views of serial adjacent sections hybridized with α_1, α_2, β_1, and β_2 rc-*erbA* probes are shown below. β_2-Transcripts are evident in P0 subiculum (*S*) and CA1. *Arrows in P11,* β_1 photomicrograph identify individual neurons at the basal margin of the dentate gyrus expressing high levels of rc-*erbA* β1 mRNA. Exposure time was 10 weeks. *CA1*, field CA1 of Ammon's horn, pyramidal layer; *CA3*, field CA3 of Ammon's horn, pyramidal layer; *DG*, dentate gyrus granular layer; *hi*, hippocampal neuroepithelium; *Hi*, hippocampal formation; *IBL*, inner blade dentate gyrus; *LV*, lateral ventricle; *S*, subiculum. Scale bars: thin bars, 1 mm; thick bars, 100 μm.

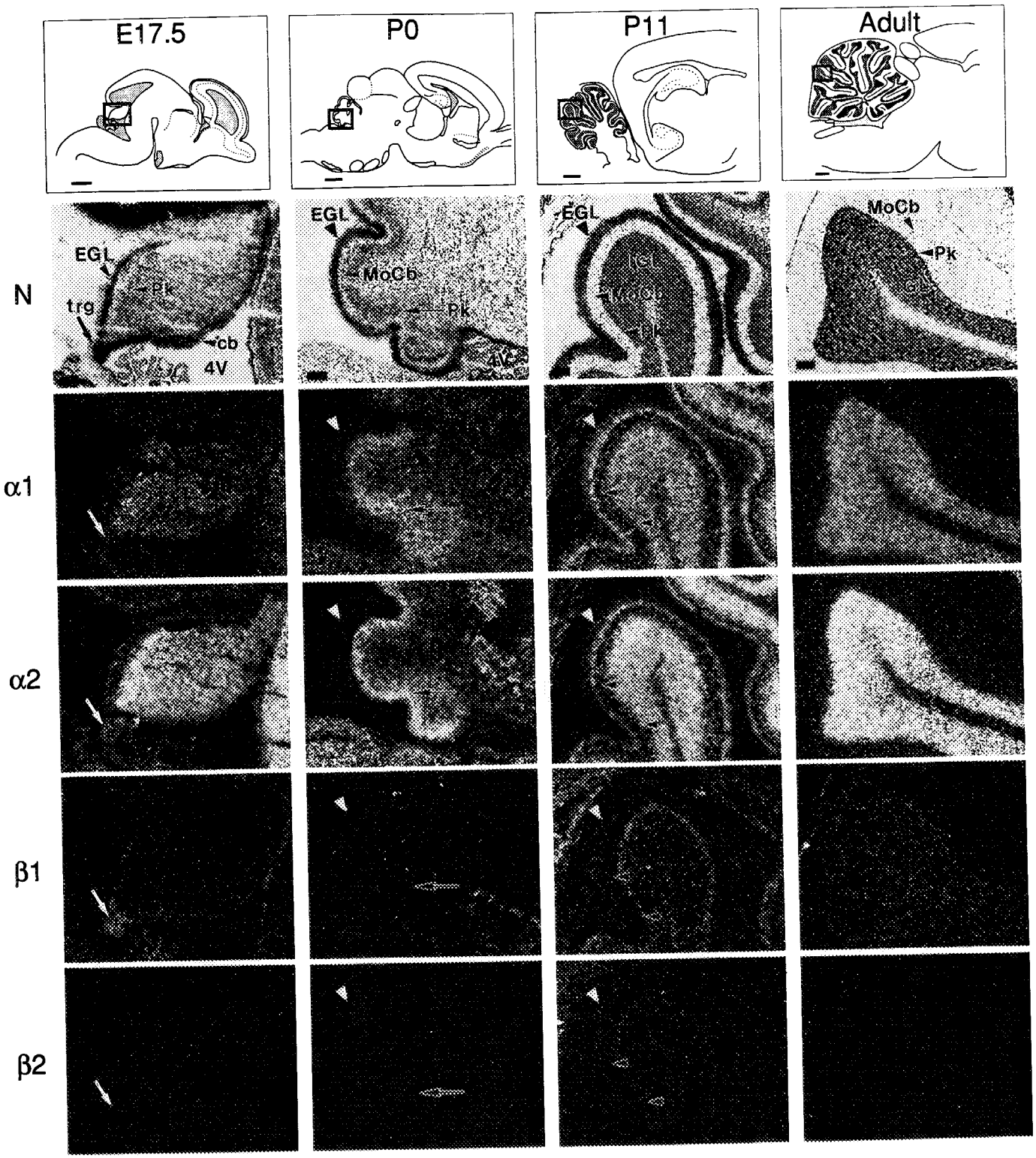

Figure 8. c-*erbA* mRNA expression in the developing cerebellar cortex. *Top row,* Schematic illustrations of sagittal sections taken from E17.5, P0, P11, and adult rat brain. Photomicrographs corresponding to *boxed areas in top row* are shown below. *Row N (Nissl),* Bright-field photomicrographs showing development of cerebellar cortical layers. *Rows* α_1, *α2, β1,* and *β2.* Dark-field photomicrographs of adjacent sections hybridized with α_1, α_2, β_1, and β_2 c-*erbA* probes. Following hybridization, sections were coated with photographic emulsion. Exposure time was 8 weeks. *4V,* fourth ventricle; *cb,* cerebellar neuroepithelium; *EGL,* external germinal layer; *IGL,* internal granular layer; *MoCb,* molecular layer of cerebellum; *Pk,* Purkinje cell layer; *trg,* germinal trigone. Scale bars: thin, 1 mm; thick, 100 μm.

cells throughout this entire region of the hypothalamus, including the PVN and anterobasal nucleus. β_1-mRNA, however, was closely associated with that portion of the PVN expressing TRH mRNA. β_2-mRNA was found at near-background levels in this area.

The distribution of α_1, α_2, and β_2-transcripts noted on E19.5 was maintained through P0, P4, P7, P11, P21 (not shown), and adulthood (Fig. 7*I–P*). During this same period, however, β_1-mRNA levels in the PVN surprisingly fell to undetectable levels by P7, only to gradually reemerge beginning on P11 (not shown). Such a temporal pattern is reminiscent of CRF mRNA expression in the PVN during the stress nonresponsive period (Grino et al., 1989). In the adult PVN, as in the fetal PVN, β_1-transcripts are found in distribution similar to that of TRH mRNA (Fig. 7*I–P*). Conclusions about a possible direct role of thyroid hormone receptors in the feedback regulation of TRH gene transcription *in vivo* await cellular colocalization studies.

Cerebellum

We first noted α_1- and α_2-mRNAs in the cerebellar neuroepithelium on E13.5 (Table 1). By E15.5, α_1- and α_2-labeling of the primordial cerebellum had intensified (Table 1). During this time (E13–E16), the cerebellar neuroepithelium, which lines the roof of the fourth ventricle, gives rise to immature but postmitotic Purkinje cells (Altman and Bayer, 1978). Migration of these cells toward the pia results in the formation of the Purkinje cell layer (Altman and Bayer, 1985). This layer is already prominently labeled by α_1- and α_2-probes on E17.5 (Fig. 8). A second cerebellar germinal zone, the external germinal layer (EGL), develops when neuroblasts from the germinal trigone (rostral rhombic lip) migrate rostrally over the surface of the cerebellum (Altman and Bayer, 1985). We first observed this migration on E15.5, and by E17.5 the EGL had very low levels of α_1- and α_2-mRNAs. β_1-mRNAs were notably concentrated in the germinal trigone at this stage. Besides supplying neuroblasts to the EGL, the germinal trigone produces neuroblasts that populate several brainstem nuclei (Jacobson, 1978). β_2-mRNAs were not found in excess of background levels in the fetal cerebellum. The overall rc-*erbA* expression pattern in the cerebellar cortex was maintained from E17.5 through P1.

An important transition in cerebellar development occurs in the first week postnatally. At this time, some neuroblasts in the rapidly proliferating EGL begin to undergo terminal mitosis (Fujita et al., 1966). The resulting postmitotic granule, basket, and stellate neurons initially collect in a layer called EGL-deep, where they prepare for inward migration (Jacobson, 1978). As seen on P11, the transition from proliferating EGL to postmitotic granule cell precursor in the EGL-deep is associated with an upregulation in α_1- and α_2-mRNA levels. In Figure 8, this can be seen as a prominent narrow strip of grains along the inner edge of the EGL. α_1- and α_2-probes also label cells within the molecular and Purkinje cell/internal granule layer (P/IGL). Highest levels of β_1- and β_2-transcripts at P11 were found in the Purkinje cell layer and the deep cerebellar neurons. The EGL dissipates around P22, and in the adult cerebellum, the P/IGL and the deep cerebellar neurons are labeled by the β_1-probe. Using oligonucleotide probes, we were previously unable to detect c-*erbAβ* mRNAs above background in the adult cerebellar cortex (Bradley et al., 1989). The high sensitivity of cRNA probes (Cox et al., 1984) allows us now to detect β_1-mRNA in the P/IGL. Thus, the present results are consistent with the recent immunocytochemical localization rc-*erbAβ*1 and rc-*erbAα*2 antigens in the cerebellar cortex (Strait et al., 1991).

Discussion

By hybridization histochemistry we have found differential expression of α_1, α_2, β_1, and β_2 rc-*erbA* mRNAs in the developing rat brain. Although rat α- and β-thyroid hormone receptors share very similar biochemical properties, including hormone and DNA binding (Glass and Holloway, 1990), the existence of two conserved c-*erbA* genes suggests distinct biological roles for the corresponding gene products. Our findings support this view.

Transcripts encoding two of the three functional mammalian thyroid hormone receptors, α_1 and β_1, have previously been found by Northern analysis and PCR in rat and human brain (Thompson et al., 1987; Koenig et al., 1988; Mitsuhashi et al., 1988; Murray et al., 1988; Nakai et al., 1988a,b; Hodin et al., 1989, 1990; Cook and Koenig, 1990). In contrast, expression of β_2-mRNA in the adult rat has been shown to occur only in the pituitary (Hodin et al., 1989, 1990; Cook and Koenig, 1990). The high sensitivity and cellular specificity of cRNA hybridization histochemistry (Cox et al., 1984) have allowed us to detect specific β_2-mRNA sequence in structures including the developing striatum and hippocampus. This finding strongly suggests that three types of thyroid hormone receptors, α_1, β_1, and β_2, contribute to transcriptional regulation in the developing rat CNS. Although we cannot conclude that the β_2-RNA species we have detected by hybridization histochemistry is identical in all brain cell types examined to that previously described in the pituitary, RNA sequences complementary to our β_2-probe are present in the developing brain. The existence of mammalian developmental-specific β-variant transcripts remains a possibility.

The overlapping distributions of α- and β-thyroid hormone receptor transcripts in structures like the neocortex and CPu indicate cellular coexpression of these mRNAs is possible. T3 receptor subtypes can form heterodimers with one another as well as with other members of the nuclear receptor family (Forman et al., 1989; Glass et al., 1989). It appears likely then that cellular coexpression of three receptors for T3 would dramatically expand the range of T3 regulation of transcription during brain development. β_2-mRNA expression in the brain also suggests that tissues other than the brain and pituitary may express β_2 T3 receptors during development.

Among the most severe abnormalities associated with developmental thyroid hormone deficiency is striatopallidal motor dysfunction that is manifested as a "proximal and axial plastic rigidity and flexion dystonia" (DeLong, 1989). This neurologic deficit prompted us to examine c-*erbA* expression in the striatum. A steep gradient of β_1- and β_2-mRNAs in the perinatal striatum was observed. Although striatal gradients of cells expressing neuropeptides, such as substance P (Gerfen and Young, 1988), have previously been noted, what regulatory role, if any, a striatal gradient of T3 receptors might play in the establishment of neuronal phenotypes is unclear.

T3 action has long been implicated in regulating neuronal differentiation. Correlates of neuronal differentiation, such as neocortical dendrite branching and cerebellar synapse density, are markedly reduced in the brains of rats made hypothyroid at birth (Eayrs, 1955; Nicholson and Altman, 1972). Expression of thyroid hormone receptor genes might therefore be expected to be prominent in differentiating neurons. The segregation of proliferating, migrating, and differentiating neurons in devel-

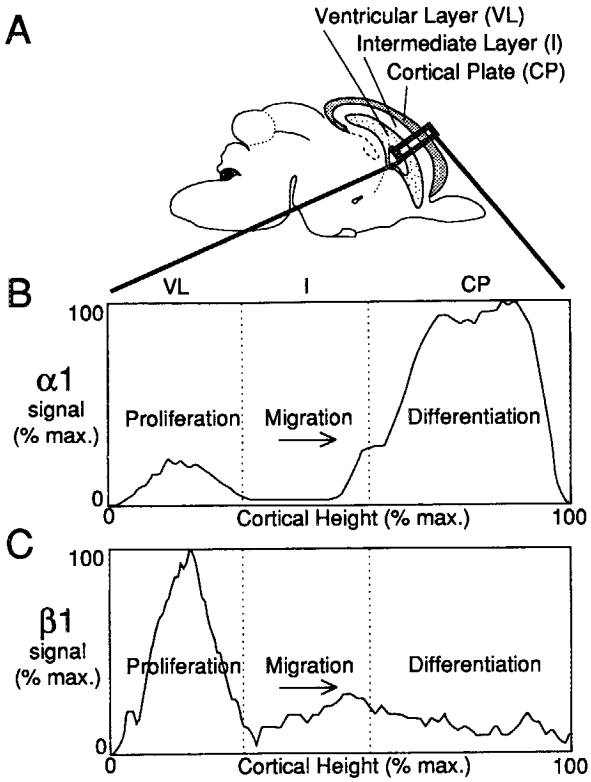

Figure 9. Differential expression of α_1- and β_1-thyroid hormone receptor transcripts in the context of cortical neuronal development. *A*, Sagittal section of E19.5 rat brain. *Boxed area* shows region used for measurements of relative levels of α_1 and β_1 c-*erbA* probe labeling of cortical layers. *B*, Representative labeling of E19.5 cortical layers by α_1 c-*erbA* cRNA probe. Typical signal on film autoradiogram of hybridized section was measured by standardized image analysis (see Materials and Methods) in region outlined in *A*. *Proliferation, migration,* and *differentiation* refer to developmental state of cortical neuroblasts and neurons in the E19.5 cerebral cortex. *Arrows* indicate direction of neuron migration. *C*, Similar to *B*, except film autoradiogram of adjacent section hybridized with c-*erbA* β_1 probe was measured.

oping laminated structures such as the cerebral cortex, hippocampus, and cerebellar cortex allowed us to test this prediction. As shown in Figure 9*B*, we found a surge in α_1-mRNA levels in fetal cortical neurons that had ceased proliferation and entered a phase of differentiation. Similar results were seen in the P11 cerebellar cortex and the fetal hippocampus. In contrast, relatively high levels of β_1-transcripts were found in proliferative zones such as the neocortical ventricular layer (Fig. 9*C*), as well as the upper tegmental neuroepithelium and the germinal trigone. Thus, in structures such as the fetal neocortex, β-thyroid hormone receptors may contribute to regulation of neuroblast proliferation, whereas α-thyroid hormone receptors may play a predominant role in neuronal differentiation.

The role of the non-T3-binding α_2-protein remains unclear. In cell culture, α_2-expression can inhibit the ability of α_1- and β_1-thyroid hormone receptors to induce T3-dependent reporter gene expression (Koenig et al., 1989). This result, combined with the extensive spatiotemporal distribution of α_2-transcripts found in the present study, suggests that widespread modulation of T3 action by α_2-proteins may occur in the developing mammalian brain. Rats made hypothyroid at birth face irreversible structural damage to their cerebral and cerebellar cortices (Schwartz, 1983). These problems can be averted if replacement thyroid hormone is given by the end of a "critical period," usually around P14 (Clos et al., 1974). A similar critical period, extending to about 3 months of age, exists for children born with congenital hypothyroidism (Frost et al., 1979). Mechanisms defining the end of the critical period are unknown. One possibility is that α_2-protein, arising at the end of the critical period, may interfere with T3 receptor function, thereby rendering the brain less responsive to T3. Our results do not support such a hypothesis since distributions of α_2-mRNAs were similar during and after the rat critical period. Therefore, the irreversibility of the effects of hypothyroidism on rat brain development are not readily explained by major shifts in α_2-mRNA expression.

Ablation of c-*erbA* in experimental animals promises to reveal exciting clues about the primary role of thyroid hormone receptors in brain development. The wide distribution of α_1-transcripts in the developing CNS suggests that targeting of c-*erbA*α may adversely affect differentiation of neurons populating multiple motor and sensory systems. Since we detect background levels of β-mRNAs over much of the α_1 spatial and temporal expression domain, β-thyroid hormone receptors may be unavailable to compensate for an ablated c-*erbA*α gene. In contrast, the highly restricted β-spatial expression domain suggests that targeting of c-*erbA*β may result in distinct neurologic deficits related to the functional derangement of regions such as neocortical layer 5, the PVN, and CA1. At all these sites, however, overlapping c-*erbA*α expression may provide α_1-thyroid hormone receptors capable of partially compensating for ablation of the c-*erbA*β gene. A lack of neurologic deficits, other than deafness, in patients homozygous for a deletion within the human c-*erbA*β gene supports this notion (Takeda et al., 1991).

Strait and colleagues have convincingly demonstrated a complex relationship between rat c-*erbA* transcript and protein levels in several rat tissues (Strait et al., 1990, 1991). The development of specific antibodies for all four rat c-*erbA* protein subtypes and combined immunocytochemistry/hybridization histochemistry should provide further insight into transcriptional and translational regulation of c-*erbA* expression during brain development. The precise role of thyroid hormone in the brain's developmental program awaits both the elucidation of those influences guiding c-*erbA* expression and the identification of neural T3 response genes.

Note added in proof: After completion of this work, Mellström et al. (1991) published a report comparing α_1 and β_1 c-*erbA* transcript distributions in the developing rat brain. Our results for α_1 and β_1 mRNAs are consistent with theirs.

References

Altman J, Bayer SA (1978) Prenatal development of the cerebellar system of the rat. I. Cytogenesis and histogenesis of the deep nuclei and the cortex of the cerebellum. J Comp Neurol 179:23–48.

Altman J, Bayer SA (1985) Embryonic development of the rat cerebellum. I. Delineation of the cerebellar primordium and early cell movements. J Comp Neurol 231:1–26.

Arriza JL, Simerly RB, Swanson LW, Evans RM (1988) The neuronal mineralocorticoid receptor as a mediator of glucocorticoid response. Neuron 1:887–900.

Bayer SA (1980) Development of the hippocampal region in the rat. II. Morphogenesis during embryonic and early postnatal life. J Comp Neurol 190:115–134.

Bayer SA (1984) Neurogenesis in the rat neostriatum. Int J Dev Neurosci 2:163–175.

Bayer SA, Yackel JW, Puri PS (1982) Neurons in the rat dentate gyrus granular layer substantially increase during juvenile and adult life. Science 216:890–892.

Bradley DJ, Young WS III, Weinberger C (1989) Differential expression of alpha and beta thyroid hormone receptor genes in rat brain and pituitary. Proc Natl Acad Sci USA 86:7250–7254.

Brent GA, Moore DD, Larsen PR (1991) Thyroid hormone regulation of gene expression. Annu Rev Physiol 53:17–35.

Burgunder JM, Taylor T (1989) Ontogeny of thyrotropin-releasing hormone gene expression in the rat diencephalon. Neuroendocrinology 49:631–640.

Clos J, Crepel F, Legrand C, Legrand J, Rabie A, Vigouroux E (1974) Thyroid physiology during the postnatal period in the rat: a study of the development of thyroid function and of the morphogenetic effects of thyroxine with special reference to cerebellar maturation. Gen Comp Endocrinol 23:178–192.

Cook CB, Koenig RJ (1990) Expression of *erbA* alpha and beta mRNAs in regions of adult rat brain. Mol Cell Endocrinol 70:13–20.

Cox KH, DeLeon DV, Angerer LM, Angerer RC (1984) Detection of mRNAs in sea urchin embryos by *in situ* using asymmetric RNA probes. Dev Biol 101:485–502.

DeLong GR (1989) Observations on the neurobiology of endemic cretinism. In: Iodine and the brain (Delong GR, Robbins J, Condliffe PG, eds), pp 231–238. New York: Plenum.

Dussault JH, Ruel J (1987) Thyroid hormones and brain development. Annu Rev Physiol 49:321–334.

Eayrs JT (1955) The cerebral cortex of normal and hypothyroid rats. Acta Anat 25:160–183.

Evans RM (1988) The steroid and thyroid hormone receptor superfamily. Science 240:889–895.

Forman BM, Yang CR, Au M, Casanova J, Ghysdael J, Samuels HH (1989) A domain containing leucine-zipper-like motifs mediate novel *in vivo* interactions between the thyroid hormone and retinoic acid receptors. Mol Endocrinol 3:1610–1626.

Forrest D, Sjoberg M, Vennström B (1990) Contrasting developmental and tissue-specific expression of alpha and beta thyroid hormone receptor genes. EMBO J 9:1519–1528.

Forrest D, Hallböök F, Persson H, Vennström B (1991) Distinct functions for thyroid hormone receptors alpha and beta in brain development indicated by differential expression of receptor genes. EMBO J 10:269–275.

Frost GJ, Parkin JM, Rowley D (1979) Congenital hypothyroidism. Lancet 2:1026.

Fujita S, Shimada M, Nakamura T (1966) H3-thymidine autoradiographic studies on the cell proliferation and differentiation in the external and the internal granular layers of the mouse cerebellum. J Comp Neurol 128:191–208.

Gerfen CR, Young WS III (1988) Distribution of striatonigral and striatopallidal peptidergic neurons in both patch and matrix compartments: an *in situ* hybridization histochemistry and fluorescent retrograde tracing study. Brain Res 460:161–167.

Glass CK, Holloway JM (1990) Regulation of gene expression by the thyroid hormone receptor. Biochem Biophys Acta 1032:157–176.

Glass CK, Lipkin SM, Devary OV, Rosenfeld MG (1989) Positive and negative regulation of gene transcription by a retinoic acid–thyroid hormone receptor heterodimer. Cell 59:697–708.

Grino M, Young WS III, Burgunder J-M (1989) Ontogeny of expression of the corticotropin-releasing factor gene in the hypothalamic paraventricular nucleus and of the proopiomelanocortin gene in rat pituitary. Endocrinology 124:60–68.

He X, Rosenfeld MG (1991) Mechanisms of complex transcriptional regulation: implications for brain development. Neuron 7:183–196.

Hebel R, Stromberg MW (1986) Anatomy and embryology of the laboratory rat. Worthsee: Biomed.

Hicks SP, D'Amato CJ (1968) Cell migrations to the isocortex in the rat. Anat Rec 160:619–634.

Hodin RA, Lazar MA, Wintman BI, Darling DS, Koenig RJ, Larsen PR, Moore DD, Chin WW (1989) Identification of a thyroid hormone receptor that is pituitary-specific. Science 244:76–79.

Hodin RA, Lazar MA, Chin WW (1990) Differential and tissue-specific regulation of the multiple rat c-*erbA* messenger RNA species by thyroid hormone. J Clin Invest 85:101–105.

Izumo S, Mahdavi V (1988) Thyroid hormone receptor alpha isoforms generated by alternative splicing differentially activate myosin HC gene transcription. Nature 334:539–542.

Jacobson M (1978) Developmental neurobiology, pp 62–88. New York: Plenum.

Koenig RJ, Warne RL, Brent GA, Harney JW, Larsen PR, Moore DD (1988) Isolation of a cDNA clone encoding a biologically active thyroid hormone receptor. Proc Natl Acad Sci USA 85:5031–5035.

Koenig RJ, Lazar MA, Hodin RA, Brent GA, Larsen PR, Chin WW, Moore DD (1989) Inhibition of thyroid hormone action by a non-hormone binding c-*erbA* protein generated by alternative mRNA splicing. Nature 337:659–661.

Koller KJ, Wolff RS, Warden MK, Zoeller RT (1987) Thyroid hormones regulate levels of thyrotropin-releasing-mRNA in the paraventricular nucleus. Proc Natl Acad Sci USA 84:7329–7333.

Lazar MA, Hodin RA, Darling DS, Chin WW (1988) Identification of a rat c-*erbA* alpha-related protein which binds deoxyribonucleic acid but does not bind thyroid hormone. Mol Endocrinol 2:893–901.

Mellström B, Naranjo JR, Santos A, Gonzalez AM, Bernal J (1991) Independent expression of the alpha and beta c-*erbA* genes in developing rat brain. Mol Endocrinol 5:1339–1350.

Mitsuhashi T, Nikodem VM (1989) Regulation of expression of the alternative mRNAs of the rat alpha-thyroid hormone receptor gene. J Biol Chem 264:8900–8904.

Mitsuhashi T, Tennyson GE, Nikodem VM (1988) Alternative splicing generates messages encoding rat c-*erbA* proteins that do not bind thyroid hormone. Proc Natl Acad Sci USA 85:5804–5808.

Murray MB, Zilz ND, McCreary NL, MacDonald MJ, Towle HC (1988) Isolation and characterization of rat cDNA clones for two distinct thyroid hormone receptors. J Biol Chem 263:12770–12777.

Nakai A, Sakurai A, Bell GI, DeGroot LJ (1988a) Characterization of a third human thyroid hormone receptor coexpressed with other thyroid hormone receptors in several tissues. Mol Endocrinol 2:1087–1092.

Nakai A, Seino S, Sakurai A, Szilak I, Bell GI, DeGroot LJ (1988b) Characterization of a thyroid hormone receptor expressed in human kidney and other tissues. Proc Natl Acad Sci USA 85:2781–2785.

Nicholson JL, Altman J (1972) Synaptogenesis in the rat cerebellum: effects of early hypo- and hyperthyroidism. Science 176:530–532.

North D, Fisher DA (1990) Thyroid hormone receptor and receptor-related RNA levels in developing rat brain. Pediatr Res 28:622–625.

Okayama H, Kawaichi M, Brownstein M, Lee F, Yokota T, Arai K (1987) High-efficiency cloning of full-length cDNA; construction and screening of cDNA expression libraries for mammalian cells. Methods Enzymol 154:3–28.

Perez-Castillo A, Bernal J, Ferreiro B, Pans T (1985) The early ontogenesis of thyroid hormone receptor in the rat fetus. Endocrinology 117:2457–2461.

Raedler E, Raedler A (1978) Autoradiographic study of early neurogenesis in rat neocortex. Anat Embryol (Berl) 154:267–284.

Raedler E, Raedler A, Feldhaus S (1980) Dynamical aspects of neocortical histogenesis in the rat. Anat Embryol (Berl) 158:253–269.

Sanger F, Nicklen S, Coulson AR (1977) DNA sequencing with chain-terminating inhibitors. Proc Natl Acad Sci USA 74:5463–5467.

Sap J, Munoz A, Damm K, Goldberg Y, Ghysdael J, Leutz A, Beug H, Vennström B (1986) The c-*erb-A* protein is a high-affinity receptor for thyroid hormone. Nature 324:635–640.

Schwartz HL (1983) Effect of thyroid hormone on growth and development. In: Molecular basis of thyroid hormone action (Oppenheimer JH, Samuels HH, eds), pp 413–444. New York: Academic.

Segerson TP, Kauer J, Wolfe HC, Mobtaker H, Wu P, Jackson IMD, Lechan RM (1987) Thyroid hormone regulates TRH biosynthesis in the paraventricular nucleus of the rat hypothalamus. Science 238: 78–80.

Simmons DM, Arriza JL, Swanson LW (1989) A complete protocol for *in situ* hybridization of messenger RNAs in brain and other tissues with radiolabelled single-stranded RNA probes. J Histotechnol 12: 169–181.

Strait KA, Schwartz HL, Perez CA, Oppenheimer JH (1990) Relationship of c-*erbA* mRNA content to tissue triiodothyronine nuclear binding capacity and function in developing and adult rats. J Biol Chem 265:10514–10521.

Strait KA, Schwartz HL, Seybold VS, Ling NC, Oppenheimer JH (1991) Immunofluorescence localization of thyroid hormone receptor protein beta1 and variant alpha2 in selected tissues: cerebellar Purkinje cells as a model for beta1 receptor-mediated developmental effects of thyroid hormone in brain. Proc Natl Acad Sci USA 88:3887–3891.

Struhl K (1991) Mechanisms for diversity in gene expression patterns. Neuron 7:177–181.

Takeda K, Balzano S, Sakurai A, DeGroot LJ, Refetoff S (1991) Screening of nineteen unrelated families with generalized resistance to thyroid hormone for known point mutations in the thyroid hormone receptor beta gene and the detection of a new mutation. J Clin Invest 87:496–502.

Thompson CC, Weinberger C, Lebo R, Evans RM (1987) Identification of a novel thyroid hormone receptor expressed in the mammalian central nervous system. Science 237:1610–1614.

Weinberger C, Thompson CC, Ong ES, Lebo R, Gruol DJ, Evans RM (1986) The c-*erb-A* gene encodes a thyroid hormone receptor. Nature 324:641–646.

Whitfield HJ, Brady LS, Smith MA, Mamalaki E, Fox RJ, Herkenham M (1990) Optimization of cRNA probe *in situ* hybridization methodology for localization of glucocorticoid receptor mRNA in rat brain: a detailed protocol. Cell Mol Neurobiol 10:145–157.

Wills KN, Zhang XK, Pfahl M (1991) Coordinate expression of functionally distinct thyroid hormone receptor alpha isoforms during neonatal brain development. Mol Endocrinol 5:1109–1119.

Yaoita Y, Brown DD (1990) A correlation of thyroid hormone receptor gene expression with amphibian metamorphosis. Genes Dev 4:1917–1924.

Young WS III (1990) *In situ* hybridization histochemistry. In: Methods for the analysis of neuronal microcircuits and synaptic interactions (Björklund A, Hökfelt T, Wouterlood FG, van den Pol A, eds), pp 481–512. New York: Elsevier.

Young WS III, Mezey E, Siegel RE (1986a) Quantitative *in situ* hybridization histochemistry reveals increased levels of corticotropin-releasing factor mRNA after adrenalectomy in rats. Neurosci Lett 70: 198–203.

Young WS III, Mezey E, Siegel RE (1986b) Vasopressin and oxytocin mRNAs in adrenalectomized and Brattleboro rats: analysis by quantitative *in situ* hybridization histochemistry. Mol Brain Res 1:231–241.